# Buoyancy induced flow and heat transfer inside a semicircular eccentric enclosure

Third International Conference on
Fluid Mechanics and Heat Transfer
Dec.15-16, 1999, Dhaka, Bangladesh

# BUOYANCY INDUCED FLOW AND HEAT TRANSFER INSIDE A SEMICIRCULAR ECCENTRIC ENCLOSURE

P. K. Das & S. Mahmud
Department of Mechanical Engineering, Bangladesh University of Engineering & Technology, BUET, Dhaka-1000, Bangladesh

## ABSTRACT

This paper presents buoyancy induced flow and heat transfer performance inside a semicircular enclosure with isothermal upper and lower surface. The differential forms of governing equations are solved using Finite-Difference method. Simulation was carried out for range of eccentricity, $\varepsilon$ = 0.2 to 0.6 at a fixed radius ratio $R_o / R_i = 2.0$. Grashof number was varied from 1.0 to $10^7$. Results of eccentric enclosure are compared with the concentric ($\varepsilon$ =0.0) semicircular enclosure with same radius ratio. Eccentricity has little dominance on heat transfer rate. But significant effect of eccentricity is observed on flow field.

## 1. INTRODUCTION

Natural convection heat transfer inside annular space, air-filled cavity or annular sector has wide application in many engineering problems. Kuhen and Goldstein [3-5] presented reviews of the available literature and experimental results in concentric and eccentric horizontal cylindrical annuli. Glakpe et. al. [6] examined effect of mixed boundary condition on heat transfer in eccentric enclosures. Yang et. al. [7] investigated steady laminar natural convection in a maximum eccentric ($\varepsilon$=1.0) horizontal annulus with different diameter ratios and three eccentric position. Some other numerical works are presented [8-9] heat transfer inside eccentric cylindrical annuli. In this paper, laminar steady natural convection heat transfer inside an enclosure bounded by two semicircular surface of different diameter is studied at concentric and three eccentric positions. Rate of heat transfer in terms of local and global Nusselt numbers are presented for different angular positions of inner semicircular surface and Grashof number respectively. Flow and thermal fields are analyzed by parametric presentation of streamlines and isotherms.

## 2. PROBLEM FORMULATION

Consider a fluid enclosed in a space bounded by two semicircular surface of radius $R_o$ and $R_i$ as shown in Fig.1. The surface of the semicircular surface are maintained at constant uniform temperatures $T_i$ and $T_o$, where $T_i > T_o$. Two horizontal surfaces that connect outer and inner semicircular surface are considered adiabatic. Assuming that the Boussinesq approximation is valid, the dimensionless equations governing the two-dimensional fluid motion may be reduced to:

$$\text{div } \mathbf{V} = 0 \tag{1}$$

$$(\mathbf{V}.\mathbf{grad})U = -\frac{\partial p}{\partial r} + \text{Ra Pr T Cos}\,? + \text{Pr}\,?_{r}\mathbf{V} \tag{2}$$

$$(\mathbf{V}.\mathbf{grad})V = -\frac{\partial p}{r\partial ?} + \text{Ra Pr T Sin}\,? + \text{Pr}\,?_{?\,r}\mathbf{V} \tag{3}$$

$$(\mathbf{V}.\mathbf{grad})T = ?_{r}T \tag{4}$$

$$? = ?_{ref}\left[1 - ß\left(T - T_{ref}\right)\right] \tag{5}$$

Where $\rho_{ref}$ is the density of the fluid at some reference temperature $T_{ref}$ and $\beta$ is the coefficient of thermal expansion. Schematic diagram of the problem under consideration

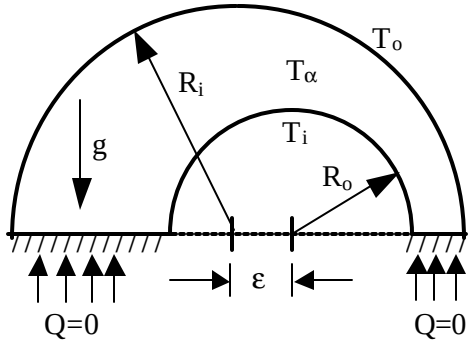


**Fig.1 Schematic diagram of problem under consideration**

is shown in Fig.1 with various geometrical parameters. The total solution domain is divided into finite number of control volume. Governing equations are then solved using control-volume-based Finite Difference method described by Chai & Patankar [1] and Patankar [2].

## 3. RESULTS AND DISCUSSIONS

Three grid sizes (30*16, 60*32, and 120*64) were chosen to carry out present simulation. Results are presented for fine grid (120*64). For a particular eccentricity, Grashof number was varied by changing dynamic viscosity keeping other fluid and geometric variables constant. Iteration was stopped when difference between two consecutive variable values for all variables fall below $10^{-5}$. For further stabilization of numerical procedure, under relaxation factor was chosen between 0.1-0.7.

### 3.1 Local heat transfer

Local Nusselt number distribution along the surface of lower semicircular surface is shown in Fig.2 for $Gr=10^2$, $10^5$. At $Gr=10^2$, heat transfer is almost invariant along the periphery of the lower semicircular surface except two corners for $\varepsilon=0.0$. At $\varepsilon=0.2$, heat transfer rate is higher than concentric case for angular position ($\theta$) between $0^O$ to $100^O$. Between $100^O$ to $180^O$ heat transfer rate is lower. For each eccentric position, there is a point on the lower semicircular surface that shows same heat transfer (intersection

point) rate of concentric case. This point shifts towards higher angular position for higher eccentricity. Interesting scenario is observed after intersection point. Heat transfer rate falls rapidly with the increase of eccentricity and minimum heat transfer occurs at higher angular position for higher eccentricity. Periodic heat transfer rate (with respect to angular position) is observe for $\varepsilon$=0.0 at Gr=$10^5$ due to symmetric multicellular flow inside the enclosure.

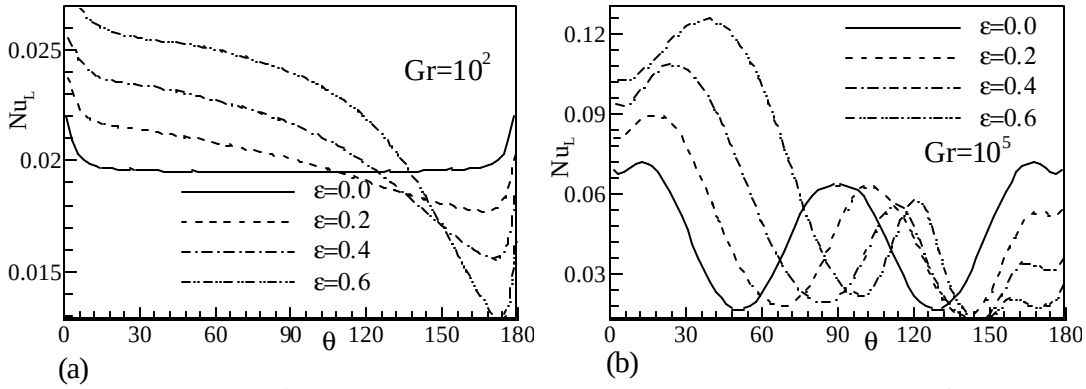


**Fig.2 Variation of local Nusselt number along lower semicircular surface, $\theta$ is measured from left to right (clockwise) over the lower semicircle**

For higher eccentricity, symmetrical nature of multicellular flow corrupts causing breakdown the periodic nature of heat transfer. This is shown in Fig.2 (b). Fig.3 shows

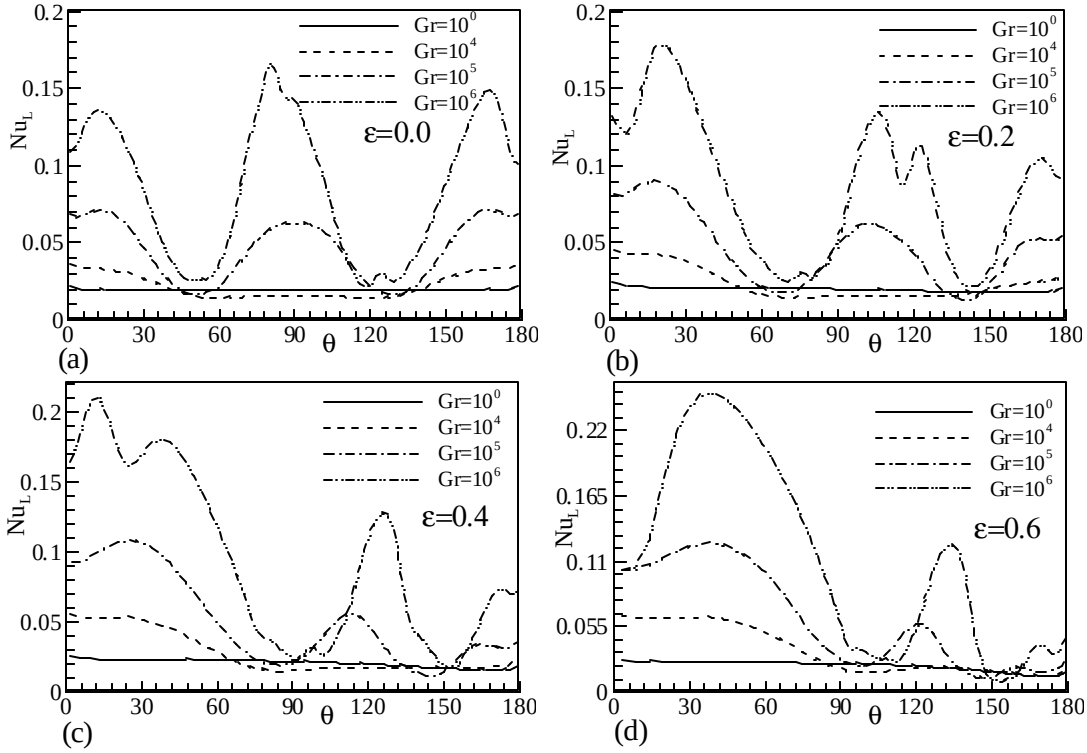


**Fig.3 Local Nusselt number distribution at fixed $\varepsilon$ and different Gr**

the Nusselt number distribution at different Grashof number for constant eccentric location.

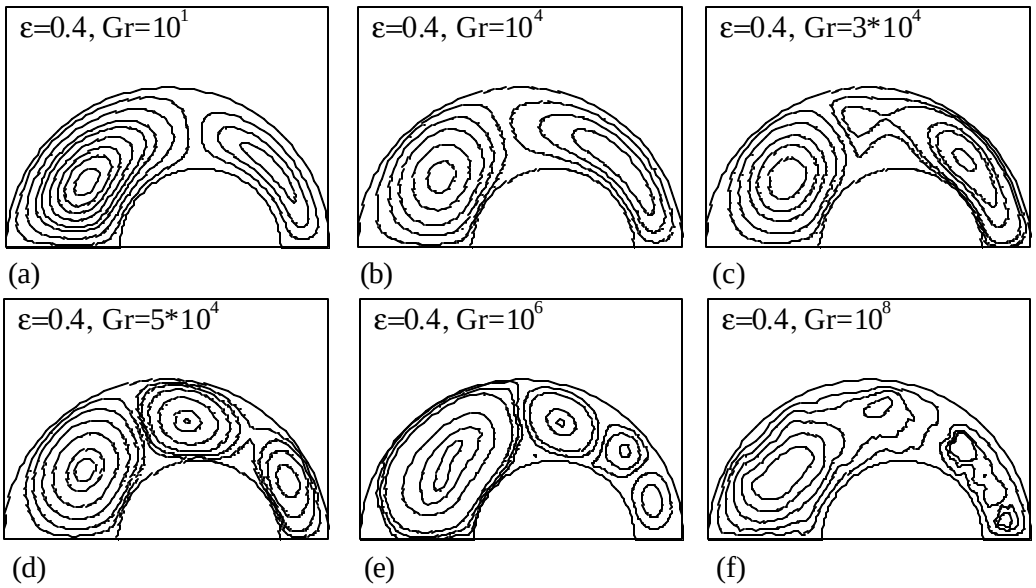


**Fig.4 Streamlines at different Grashof number for ε=0.4**

### 3.2 Flow field

Fig.4 shows the constant streamfunction contours at six different Grashof number for $\varepsilon=0.4$. At $Gr=10^1$, bicellular flow is observed with one crescent-shape vortex at narrower cross section. Size of this vortex increases with larger core at $Gr=10^4$ reducing the size of vortex at larger cross section. Bicellular flow turns into tricellular in between $Gr=3*10^4 - 5*10^4$. At $Gr=10^6$, multicellular flow with three small vortex at narrower cross section and one large vortex at larger cross section is observed. Instability in hydrodynamic boundary layer at narrower cross section breaks the crescent-shape vortex into three separate small circular zones. The distorted streamlines at $Gr=10^8$ indicate transition to turbulence. Fig.5 shows the effect of eccentricity on flow field at

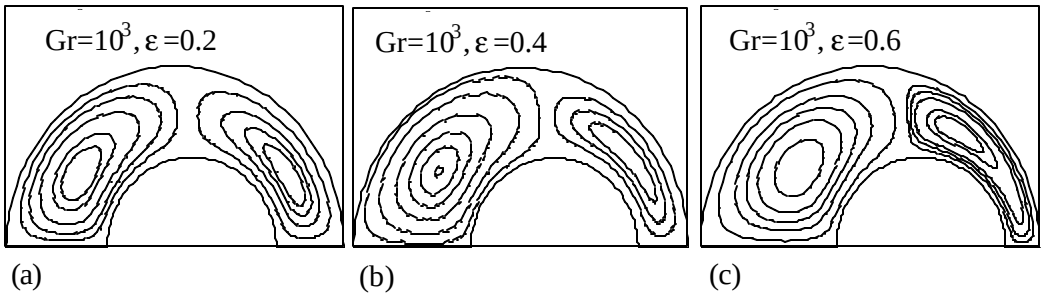


**Fig.5 Streamlines at different eccentricity & constant Grashof number**

constant Grashof number $10^3$. Higher eccentricity shifts the core of crescent-shape vortex of narrower cross section upward. The vortex of larger cross section remains unchanged with the increase of eccentricity.

### 3.3 Thermal field

Isothermal lines in Fig.6 present the thermal field for ε=0.4. At Gr=10, buoyancy effect is almost negligible. Isothermal lines are semicircular in shape showing uniform temperature gradient normal to the lower semicircular surface. Isothermal lines concentrated near the left most corner of the inner semicircular surface showing higher

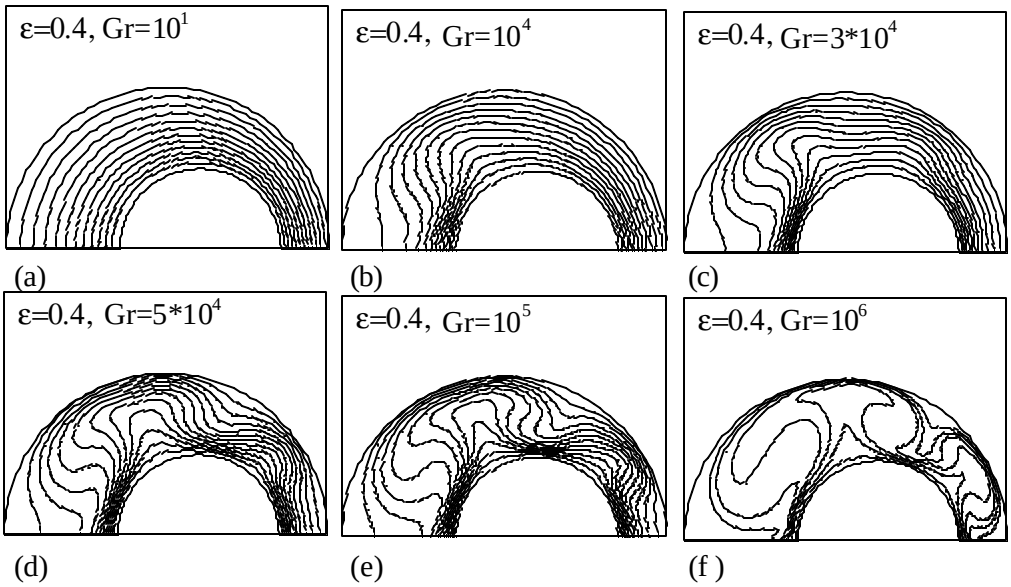


**Fig.6 Isothermal lines at different Grashof numbers for ε=0.4**

temperature gradient. Other parts of the enclosure show uniform distribution of isothermal lines. Transition to tricellular flow change the isotherms pattern at $Gr=3*10^4$. Clear three spots of high near wall temperature gradient normal to the inner semicircular surface is observed at $Gr=5*10^4$ (Fig.6d). Heat transfer rates higher at these spots. Similar pattern is observed at $Gr=10^5$ but temperature gradient is higher than previous case. At $Gr=10^6$, the hot plume of the temperature pattern is developed fully and a portion of isotherms becomes swirl shown in Fig.6 (f). This is due to present of multicellular flow pattern.

### 4. CONCLUSIONS

Buoyancy induced flow and heat transfer inside a semicircular eccentric enclosure is investigated numerically. Eccentricity affects both local heat transfer pattern and flow field. Introducing eccentricity changes the true periodic pattern of local heat transfer of concentric enclosure. But eccentricity has little influence on average heat transfer rate. Crescent-shape vortex is observed at smaller cross sectional area at lower Grashof number, which distorted into bicellular and then into multicellular pattern at higher Grashof number. But the vortex of larger cross sectional area remains almost unchanged with the increase of Grashof number.

## NOMENCLATURE

| | | | |
|---|---|---|---|
| $g$ | = gravity vector | $T_{ref}$ | = reference temperature |
| $Gr$ | = Grashof number, $(\rho^2 g\beta\Delta T\, R_o/\mu^2)$ | $Q$ | = heat transfer rated |
| $h$ | = convective heat transfer coeff. | | |
| $K_f$ | = thermal conductivity of fluid | *Greek symbol* | |
| $Nu_L$ | = local Nusselt number, $(h\, R_o/K_f)$ | $\beta$ | = thermal expansion coefficient |
| $Nu_{av}$ | = average Nusselt number | $\varepsilon$ | = eccentricity |
| $p$ | = pressure | $\mu$ | = dynamic viscosity |
| $R_i$ | = radius of inner semicircle | $\rho$ | = mass density |
| $R_o$ | = radius of outer semicircle | $\theta$ | = angular position |
| $T_i$ | = inner wall temperature | $\Delta_{r,\theta}$ | = Laplacian symbol |
| $T_\alpha$ | = fluid temperature | | |

## REFERENCE


[1] J. C. Chai, S. V. Patankar, Laminar natural convection in internally finned horizontal annuli, Numerical Heat Transfer, vol.24,1993

[2] S. V. Patankar, Numerical heat transfer and fluid flow, McGraw-Hill, New York, 1980

[3] T. H. Kuhen, R. J. Goldstein, An experimental and theoretical study of natural convection in the annulus between horizontal concentric cylinders, J. Fluid Mech. vol. 74, 1976

[4] T. H. Kuhen, R. J. Goldstein, An experimental study of natural convection heat transfer in concentric and eccentric horizontal cylindrical annuli, J. Heat Transfer, vol. 100, 1978

[5] T. H. Kuhen, RJ Goldstein, A parametric study of Prandtl number and diameter ratio effects on natural convection heat transfer in horizontal cylindrical annulus, J. Heat Transfer, vol. 102, 1980

[6] E. K. Glakpe, C. B. Watkins, Effect of mixed boundary conditions on natural convection in concentric and eccentric annular enclosure, AIAA Paper, 1987

[7] Z. Yang, J. He, A study of natural convection heat transfer in a maximum eccentric horizontal annulus, Proc. Of 11th IHTC, vol. 3, 1998

[8] C. H. Cho, K. S. Chang, K. H. Park, Numerical simulation of natural convection in concentric and eccentric horizontal annuli, ASME, J. of Heat Transfer, vol. 104, 1982

[9] J. Prusa, L. S. Yao, Natural convection heat transfer between eccentric horizontal cylinders, ASME, J. of Heat Transfer, vol. 105, 1983